

Article

High Light Intensity and CO₂ Enrichment Synergistically Mitigated the Stress Caused by Low Salinity in *Pyropia yezoensis*

Hailong Wu^{1,2,*}, Chuchu Wang^{1,2}, He Li^{1,2}, Jiang Chen^{1,2}, Jiankai Zhang^{1,2}, Zixue Luo^{1,2}, Fangsheng Cheng^{1,2} and Juntian Xu^{1,2}

¹ Jiangsu Key Laboratory of Marine Bioresources and Environment, Jiangsu Ocean University, Lianyungang 222005, China; 2021210115@jou.edu.cn (C.W.); lihe@jou.edu.cn (H.L.); 2022210127@jou.edu.cn (J.Z.); 2022220135@jou.edu.cn (Z.L.); 2022220803@jou.edu.cn (F.C.); jtxu@jou.edu.cn (J.X.)

² Co-Innovation Center of Jiangsu Marine Bio-Industry Technology, Jiangsu Ocean University, Lianyungang 222005, China

* Correspondence: hlwu@jou.edu.cn; Tel./Fax: +86-(0)-159-5074-4506

Abstract: Macroalgae, playing a crucial role in coastal marine ecosystems, are subject to multiple environmental challenges due to tidal and seasonal alterations. In this work, we investigated the physiological responses of *Pyropia yezoensis* to ocean acidification (ambient CO₂ (AC: 400 μatm) and elevated CO₂ (HC: 1000 μatm)) under changing salinity (20, 30 psu) and light intensities (50, 100 μmol photons m⁻² s⁻¹) by measuring the growth, pigment content, chlorophyll fluorescence, and soluble sugar content. The key results are the following: (1) *P. yezoensis* exhibited better growth under normal salinity (30 psu) compared to hyposaline conditions (20 psu). (2) Intermediate light intensity increased phycoerythrin content, ultimately enhancing thalli growth without significant changes to the contents of chlorophyll *a* and carotenoids. (3) Ocean acidification alleviated hyposaline stress by enhancing pigment production in *P. yezoensis* only at a salinity of 20 psu, highlighting the complex interplay of these environmental factors. These findings indicate that higher light intensities and elevated pCO₂ levels could mitigate the stress caused by low salinity.



Citation: Wu, H.; Wang, C.; Li, H.; Chen, J.; Zhang, J.; Luo, Z.; Cheng, F.; Xu, J. High Light Intensity and CO₂ Enrichment Synergistically Mitigated the Stress Caused by Low Salinity in *Pyropia yezoensis*. *J. Mar. Sci. Eng.* **2023**, *11*, 2193. <https://doi.org/10.3390/jmse11112193>

Academic Editor: Alberto Barausse

Received: 19 October 2023

Revised: 11 November 2023

Accepted: 12 November 2023

Published: 17 November 2023



Copyright: © 2023 by the authors. Licensee MDPI, Basel, Switzerland. This article is an open access article distributed under the terms and conditions of the Creative Commons Attribution (CC BY) license (<https://creativecommons.org/licenses/by/4.0/>).

Keywords: *Pyropia yezoensis*; growth; high CO₂ level; light intensity; salinity

1. Introduction

Marine macroalgae have been recognized as a crucial group of organisms for sustaining coastal ecosystems [1]. Although macroalgae cover only a minute part of the oceans, they contribute 5–10% of the total oceanic primary productivity [1,2]. In addition to their pivotal role in carbon fixation and sequestration [3], macroalgae also serve as a source of food, medicine, and biofuel for humankind [4,5]. *Pyropia yezoensis*, previously known as *Porphyra yezoensis* [6], is a red alga belonging to *Rhodophyta*. In particular, *P. yezoensis* inhabits the rocky intertidal zone, where environmental conditions such as light intensity, CO₂ concentration, nutrients, and salinity are highly variable due to tidal changes and terrestrial runoffs. Given its considerable economic and ecological value [7], *P. yezoensis* has been extensively cultivated in shallow areas of China, Korea, and Japan [8]. Recently, much more attention has been given to the growth and photosynthesis of *P. yezoensis* because of its close relationship with crop yield [9,10].

Due to fossil fuel burning and other anthropogenic activities, atmospheric CO₂ concentrations have been continuously rising since the industrial revolution and exceed 410 ppm in the present day [11]. The absorption of anthropogenic CO₂ by the oceans has led to a decrease in seawater pH and substantial variations in other seawater carbonate chemistries, a process known as ocean acidification (OA) [12]. It is expected that the mean pH of the

global surface ocean will further decrease by 0.3–0.4 units by the end of the century based on Representative Concentration Pathway (RCP) 8.5 [12,13]. The effect of OA in coastal waters is more serious than that in pelagic systems due to the reduced buffering ability associated with an additional decline in pH [14]. Ocean acidification could directly and indirectly influence the physiology, life cycles, and community structures of macroalgae [15,16]. Previous studies have shown that ocean acidification has a negative effect on fleshy and calcareous seaweeds, which could reduce the calcification rate of calcifying organisms due to a declined CO_3^{2-} concentration and thus threaten their survival [17]. The decrease in relative growth rates has also been observed in *Saccharina japonica* and *Grateloupia filicina* when the $p\text{CO}_2$ levels exceed 700 μatm [18]. However, elevated $p\text{CO}_2$ has positive effects on the photosynthesis or growth of marine red macroalgae (*Gracilaria* sp., *G. chilensis*, and *G. lemaneiformis*) [19,20].

It is well-known that light is one of the major prerequisites for the photosynthesis of macroalgae. Light drives photosynthesis to produce carbohydrates to support metabolism and growth [21]. At low light levels, photosynthesis and growth are positively related to light intensity, but above saturating light intensity, photoinhibition in algae occurs [22]. Excess photon energy absorbed by pigments compels algae to produce large amounts of reactive oxygen species (ROS), which causes photodamage to the algae and ultimately inhibits growth [23,24]. Furthermore, light can also regulate the effects of ocean acidification. Elevated $p\text{CO}_2$ promotes the growth rate of *P. yezoensis* under light-limiting conditions due to the reallocated energy saved by the down-regulation of CO_2 -concentrating mechanisms (CCMs), whereas it exacerbates the inhibition of photosynthesis in *P. yezoensis* at a high light intensity [25,26]. Salinity variation, as a local environmental factor, tends to exhibit strong fluctuations ranging from 17 to 40 psu due to runoff, precipitation, and evaporation [27,28]. Salinity can alter the osmotic pressure within algal cells and affect ionic switches in membranes [29]. Hence, macroalgae need to reallocate the available energy to the osmotic regulation process to survive under fluctuating salinity conditions, which results in a strong inhibition of the growth of most macroalgae [28]. It has been reported that the growth, photosynthesis, and antioxidant activity of macroalgae decreased under salinity-induced stress [29,30]. Compared to high salinity levels, low salinities induce more serious oxidative damage, which negatively affects intertidal macroalgal growth, such as *Gracilaria*, *Ulva*, and *Pyropia* [29,31,32].

To our knowledge, most of the previous studies focused on a single or two environmental factors, while little is known about the interactive effects of salinity, light intensity, and CO_2 concentrations on *P. yezoensis*. The ocean is a complex ecosystem where environmental factors change concurrently. *P. yezoensis*, as a macroalgae living in the intertidal zone, is bound to be affected by these environmental changes. In this study, *P. yezoensis* alga were selected to investigate their physiological responses to the combined effects of OA with two salinity and light intensity levels. This study could provide helpful insights into how *P. yezoensis* will respond to climate changes in the future.

2. Materials and Methods

2.1. Collection and Culture Conditions

Pyropia yezoensis was collected from the Gaogong islands, Lianyungang, China (34°54'31" N; 119°31'57" E). The thalli of *P. yezoensis* (4–5 cm in length) was brought back to the laboratory in a cooling box within 2 h and cleaned using sterile seawater to remove sediments and impurities. Healthy thalli were selected and pre-cultured for about 1 week in 1000 mL bottles containing filtered natural seawater with Provasoli enriched seawater medium (PES) [33], were aerated continuously, and the seawater medium was changed every day. The thalli were cultured under 100 $\mu\text{mol photons m}^{-2} \text{ s}^{-1}$ of photosynthetically-active radiation (PAR) with a 12 h:12 h (light/dark) photoperiod at 10 °C in an intelligent illumination incubator (Jiangnan GXZ-300C, Ningbo, China).

2.2. Experimental Design

After the pre-culture period, algae samples (fresh weight, FW) were selected randomly, and 0.01 g were cultured in 1000 mL bottles containing artificial seawater enriched with PES medium. We considered 20 psu as low salinity (LS) and 30 psu as high salinity (HS) to simulate the cultivation area conditions of *P. yezoensis* near and far from the estuary in Lianyungang. Different salinity treatments were prepared by diluting artificial seawater with distilled water. Considering the relatively high turbidity of the coastal seawater aquaculture area, two light intensity levels of 50 $\mu\text{mol photons m}^{-2} \text{s}^{-1}$ (low irradiance, LI) and 100 $\mu\text{mol photons m}^{-2} \text{s}^{-1}$ (intermediate irradiance, II) were set in this study. Two CO_2 concentrations of 400 μatm (ambient CO_2 , AC) and 1000 μatm (elevated CO_2 , HC) were also set for $p\text{CO}_2$ treatments. The ambient CO_2 and elevated CO_2 were continuously provided by pumping outdoor air and generated with a CO_2 plant incubator (HP 1000 GD, Wuhan Ruihua Instrument and Equipment Ltd., Wuhan, China), respectively. All treatments were performed in three replicates for 10 days, and were renewed every 2 days with fresh PES medium. The other culture conditions were the same as the pre-acclimation conditions. All parameters (chlorophyll fluorescence and pigment contents) were measured at the end of the culture period for each treatment.

2.3. Carbonate Chemistry System

To determine the stability of the carbonate system in cultures, pH was measured using a pH meter (FE22-Meter/FE22-Standard, Mettler Toledo, Shanghai, China), which was three-point calibrated with a standard National Bureau of Standards (NBS) buffer. The total alkalinity (TA) was measured using acidimetric titration [34]. Other parameters of the carbonate system were calculated from pH and TA data with CO2SYS software [35]. All of the carbonate chemistry parameters are shown in Table 1.

Table 1. Carbonate chemistry parameters in the cultures of *Pyropia yezoensis* exposed to different salinities (20 and 30 psu) at different light intensities (50, 100 $\mu\text{mol photons m}^{-2} \text{s}^{-1}$) treated with AC and HC conditions (AC, 400 $\mu\text{atm CO}_2$; HC, 1000 $\mu\text{atm CO}_2$). The values are means \pm SD of triplicate cultures. Different superscripted letters indicate significant ($p < 0.05$) differences among the treatments.

Treatment	pH	TA (μM)	HCO_3^- (μM)	CO_3^{2-} (μM)	CO_2 (μM)	DIC (μM)
LS-50-AC	8.08 \pm 0.06 ^a	1555.8 \pm 92.9 ^a	1355.0 \pm 100.1 ^a	80.38 \pm 6.31 ^a	11.96 \pm 2.21 ^a	1447.4 \pm 100.1 ^a
LS-100-AC	8.07 \pm 0.01 ^a	1551.6 \pm 66.0 ^a	1352.8 \pm 60.5 ^a	79.61 \pm 3.47 ^a	11.92 \pm 0.71 ^a	1444.3 \pm 64.0 ^a
HS-50-AC	8.12 \pm 0.01 ^a	2034.0 \pm 49.0 ^b	1670.1 \pm 37.4 ^b	144.99 \pm 5.88 ^b	11.56 \pm 0.24 ^a	1826.6 \pm 42.8 ^b
HS-100-AC	8.11 \pm 0.01 ^a	2010.6 \pm 150.3 ^b	1659.3 \pm 131.0 ^b	139.62 \pm 10.36 ^b	11.85 \pm 1.08 ^a	1810.8 \pm 141.8 ^b
LS-50-HC	7.71 \pm 0.01 ^c	1464.8 \pm 33.8 ^a	1376.4 \pm 32.2 ^a	34.90 \pm 0.95 ^c	28.14 \pm 0.83 ^b	1439.5 \pm 33.7 ^a
LS-100-HC	7.72 \pm 0.02 ^c	1426.3 \pm 30.2 ^a	1336.8 \pm 28.3 ^a	35.16 \pm 1.92 ^c	26.37 \pm 1.05 ^b	1398.3 \pm 29.6 ^a
HS-50-HC	7.82 \pm 0.02 ^d	1902.4 \pm 9.5 ^b	1713.8 \pm 10.0 ^b	74.00 \pm 2.41 ^a	23.87 \pm 0.93 ^b	1811.7 \pm 9.9 ^b
HS-100-HC	7.82 \pm 0.01 ^d	1917.9 \pm 11.6 ^b	1726.8 \pm 10.4 ^b	75.12 \pm 1.74 ^a	23.86 \pm 0.59 ^b	1825.8 \pm 11.0 ^b

2.4. Measurement of Growth Rate

The fresh weight (FW) was measured every two days at the same time after blotting the thalli with paper towels. At the eighth day, the excess biomass was dissected out to maintain the same biomass of each group at 0.04 g. Finally, the relative growth rate (RGR) was calculated using the following equation:

$$\text{RGR} (\% \text{d}^{-1}) = \frac{\ln W_{10} - \ln W_8}{2} \times 100, \tag{1}$$

where W_{10} and W_8 represent the fresh weights measured at the 10th and 8th day, respectively.

2.5. Measurement of Chlorophyll Fluorescence

The chlorophyll fluorescence parameters of *P. yezoensis* were measured using an AquaPenin-C Chlorophyll Fluorometer (AP-C100, Photon Systems Instruments, Berlin, Germany). The saturation pulse was set at 5000 $\mu\text{mol photons m}^{-2} \text{s}^{-1}$ and lasted for 600 ms. Prior to measurement, the thalli samples were initially cut into small segments and subsequently cultured under experimental conditions for at least one hour of light repair. The rapid light curve (RLC) was measured under 8 different actinic light intensities (0, 10, 20, 50, 100, 300, 500, and 1000 $\mu\text{mol photons m}^{-2} \text{s}^{-1}$). The relative electron transport rate (rETR) was calculated as follows [36]:

$$\text{rETR} \left(\mu\text{mol e}^{-1} \text{m}^{-2} \text{s}^{-1} \right) = \text{yield} \times 0.5 \times \text{PAR}, \quad (2)$$

where yield is the effective photochemical quantum yield at each actinic light intensity; 0.5 is the theoretical ratio of the absorbed total incident light allocated to PSII; and PAR is the actinic light intensity ($\mu\text{mol photons m}^{-2} \text{s}^{-1}$). The rapid light curves of rETR were fitted with the formula as follows [37]:

$$\text{rETR} = I / (aI^2 + bI + c), \quad (3)$$

where I is light intensity ($\mu\text{mol photons m}^{-2} \text{s}^{-1}$); and a , b , and c are constant parameters. The initial slope (α), the maximum relative electron transport rate (rETR_{max}), and the saturating light intensity (I_k) were calculated according to the following equations [38]:

$$\alpha = 1/c; \quad (4)$$

$$\text{rETR}_{\text{max}} = 1 / (b + 2\sqrt{a \cdot c}); \quad (5)$$

$$I_k = c / (b + 2\sqrt{a \cdot c}). \quad (6)$$

2.6. Measurement of Pigment Contents

Chlorophyll a and carotenoids were extracted and estimated based on the method developed by Wellburn [39]. Briefly, approximately 0.02 g FW of thalli were extracted with 5 mL methanol (100%) solution at 4 °C for 24 h in darkness. After the centrifugation at 5000 $\times g$ for 5 min, the supernatant was measured using an ultraviolet spectrophotometer (UV-1800, Shimadzu, Japan) at 666, 653, and 470 nm. The contents of chlorophyll a (Chl a , mg g FW⁻¹) and carotenoids (Car., mg g FW⁻¹) were calculated using the following equation:

$$\text{Chl } a = 16.29 \times OD_{666} - 8.54 \times OD_{653}; \quad (7)$$

$$\text{Car} = (1000 \times OD_{470} + 1403.57 \times OD_{666} - 3473.87 \times OD_{653}) \div 221. \quad (8)$$

The phycoerythrin of *P. yezoensis* samples was extracted using a method based on Beer and Eshel [40]. Approximately 0.02 g fresh weight of *P. yezoensis* was homogenated and extracted with 0.1 M phosphate buffer (pH 6.8), and then centrifuged at 5000 $\times g$ for 15 min. The supernatants of the extracts were scanned at 593, 564, and 455 nm to determine the phycoerythrin content (PE, mg g FW⁻¹) according to the following equation:

$$\text{PE} = [(OD_{564} - OD_{592}) - (OD_{455} - OD_{592})] \times 0.12. \quad (9)$$

2.7. Measurement of Soluble Carbohydrates Content

The anthrone sulfuric acid colorimetric method was used to determine the concentration of soluble carbohydrates [41]. Approximately 0.02 g of fresh thalli of *P. yezoensis* were homogenized in 5 mL phosphate buffer and boiled for 1 h. After centrifugation at 5000 $\times g$

for 10 min, 1 mL supernatant was added to 3 mL 0.2% anthrone sulfuric acid solution (2 g L^{-1}). The mixture was heated at $100 \text{ }^\circ\text{C}$ for 10 min, and the absorbance was recorded at 620 nm after cooling to room temperature. The content of soluble carbohydrates (SC, mg g FW^{-1}) was calculated using the equation described below:

$$\text{Carbohydrate} = (\text{OD}_{620} - 0.0072) / 0.039. \quad (10)$$

2.8. Data Analysis

Data were analyzed using the Origin 2017 and SPSS 25.0 software programs and expressed as the means \pm standard deviation of three independent replicates. Three-way ANOVA was used to analyze the interactive effects of light intensity, salinity, and CO_2 concentrations on the relative growth rate, chlorophyll fluorescence, photosynthetic pigments, and soluble carbohydrate contents. Tukey's honest significant difference (Fisher LSD) was used for post hoc investigation. The significance level was set to 0.05.

3. Results

3.1. Growth Rate

The relative growth rate (RGR) of *P. yezoensis* was significantly influenced by light intensity ($p < 0.001$) and salinity ($p = 0.006$) (Table S1). Compared to the LI conditions ($50 \mu\text{mol photons m}^{-2} \text{ s}^{-1}$), II treatments increased the RGR of thalli significantly regardless of salinities and CO_2 concentrations. As shown in Figure 1, in the ACLS, ACHS, HCLS, and HCHS treatments, RGR was significantly enhanced by 72.7%, 75.5%, 64.1%, and 49.7% under II conditions compared with those under LI, respectively ($p < 0.001$, $p < 0.001$, $p < 0.001$, $p < 0.001$). Furthermore, under AC and HC conditions, a declined tendency in RGR was observed with the decreased salinity level (30 psu) regardless of light intensities (Figure 1, $p = 0.006$). However, no significant effect of elevated $p\text{CO}_2$ or its interaction effect with light intensity and salinity levels was observed (Table S1; $p = 0.648$, $p = 0.593$, $p = 0.633$).

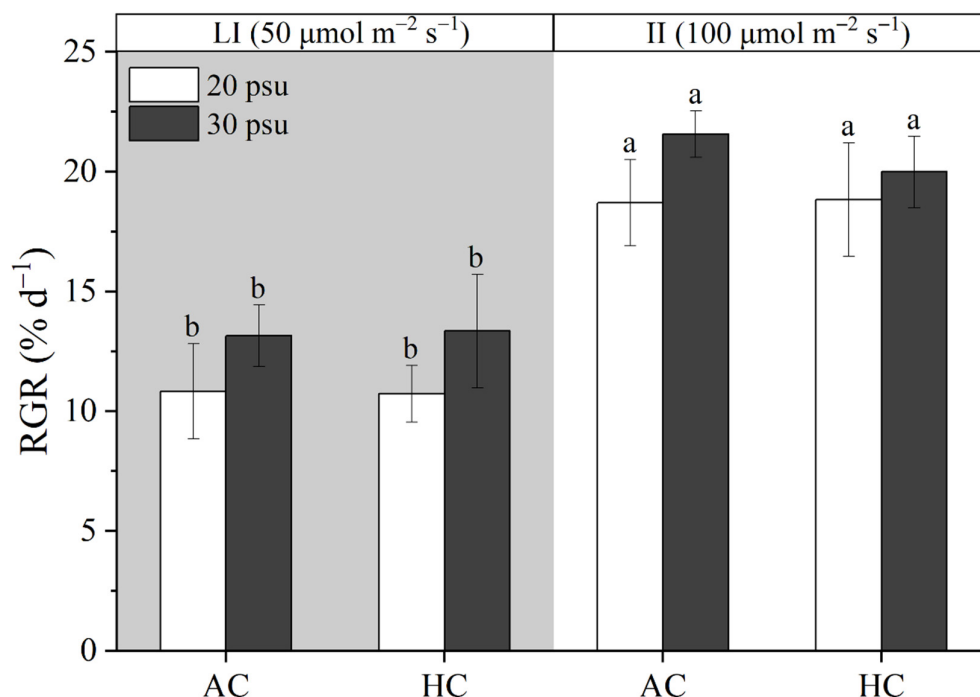


Figure 1. Changes in relative growth rate (RGR) of *Pyropia yezoensis* exposed to different salinities (20 and 30 psu) at different light intensities (50 , $100 \mu\text{mol photons m}^{-2} \text{ s}^{-1}$) treated with AC and HC conditions (AC, $400 \mu\text{atm CO}_2$; HC, $1000 \mu\text{atm CO}_2$). Results are expressed as the means \pm SD ($n = 3$). Different letters indicate significant differences ($p < 0.05$) among the treatments.

3.2. Chlorophyll a Fluorescence

The effects of CO₂ concentrations and light intensity on the rapid light curves (RLCs) of *P. yezoensis* at 20 and 30 psu are shown in Figure 2. The maximum relative electron transfer rate (rETR_{max}), light energy utilization efficiency (α), and saturated light intensity (I_k) of *P. yezoensis* were derived from the RLCs (Table 2 and Figure 2).

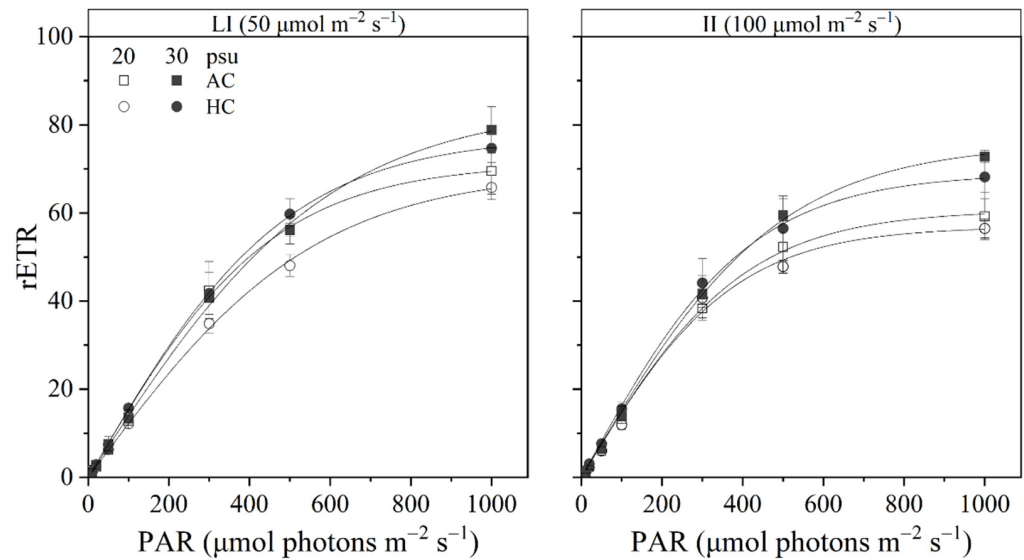


Figure 2. Rapid light curves (RLCs) of photosystem II (PSII) of *Pyropia yezoensis* exposed to different salinities (20 and 30 psu) at different light intensities (50, 100 $\mu\text{mol photons m}^{-2} \text{s}^{-1}$) treated under AC and HC conditions (AC, 400 $\mu\text{atm CO}_2$; HC, 1000 $\mu\text{atm CO}_2$) during the experiment. Data are the means \pm SD (n = 3).

Table 2. The maximum relative electron transfer rate (rETR_{max}), light energy utilization efficiency (α), and saturated light intensity (I_k) of chlorophyll fluorescence parameters in the cultures of *Pyropia yezoensis* exposed to different salinities (20 and 30 psu) at different light intensities (50, 100 $\mu\text{mol photons m}^{-2} \text{s}^{-1}$) treated under AC and HC conditions (AC, 400 $\mu\text{atm CO}_2$; HC, 1000 $\mu\text{atm CO}_2$), derived from the rapid light curves (Figure 2). The values are the means \pm SD of triplicate cultures. Different superscripted letters indicate significant ($p < 0.05$) differences among the treatments.

Treatment	rETR _{max}	α	I _k
LS-50-AC	71.17 \pm 3.82 ^{ab}	0.16 \pm 0.02 ^a	458.0 \pm 24.4 ^{be}
LS-100-AC	60.57 \pm 6.11 ^d	0.15 \pm 0.01 ^a	400.0 \pm 16.7 ^{ce}
HS-50-AC	85.02 \pm 8.34 ^a	0.14 \pm 0.01 ^{ac}	605.8 \pm 94.5 ^a
HS-100-AC	75.75 \pm 1.59 ^{bc}	0.16 \pm 0.01 ^a	488.1 \pm 13.9 ^{bef}
LS-50-HC	69.42 \pm 3.22 ^{bc}	0.12 \pm 0.01 ^{bc}	564.6 \pm 29.1 ^{af}
LS-100-HC	57.31 \pm 2.88 ^d	0.15 \pm 0.02 ^a	386.1 \pm 83.8 ^{de}
HS-50-HC	77.50 \pm 2.71 ^{ac}	0.16 \pm 0.02 ^a	495.7 \pm 35.3 ^b
HS-100-HC	69.11 \pm 5.93 ^b	0.17 \pm 0.02 ^a	418.5 \pm 50.7 ^{be}

pCO₂, light, and salinity had significant effects on the rETR_{max} (Table S2; $p = 0.027$, $p < 0.001$, $p < 0.001$, respectively). At 20 psu salinity, II treatment significantly decreased the rETR_{max} by 14.9% ($p = 0.016$) and 17.4% ($p = 0.031$) under AC and HC compared to those under the LI condition. At 30 psu salinity, rETR_{max} in the II treatment was significantly decreased by 10.9% ($p = 0.016$) and 10.8% ($p = 0.031$) under AC and HC compared to those under the LI condition, respectively. Moreover, low salinity (20 psu) decreased the rETR_{max} by 16.3%, 20.0%, and 17.1% in the ACLI, ACII, and HCII groups, respectively ($p = 0.003$, $p = 0.001$, $p = 0.008$).

Light, salinity, and the interaction between $p\text{CO}_2$ and salinity had significant effects on I_k (Table S2; $p < 0.001$, $p = 0.032$, $p = 0.006$, respectively). Elevated $p\text{CO}_2$ increased the I_k significantly under the LI condition at salinities of 20 psu and 30 psu ($p = 0.023$, $p = 0.020$, respectively). Although the intermediate irradiance decreased the I_k at each treatment, a significant difference was observed in both the HCLS and ACHS conditions, with a decline of 31.6% ($p = 0.001$) and 19.34% ($p = 0.014$), respectively. Furthermore, I_k was lower at a salinity of 20 psu than 30 psu under LI and elevated $p\text{CO}_2$ conditions ($p = 0.003$).

Only the interaction between $p\text{CO}_2$ and salinity had significant effects on α (Table S2, $p = 0.033$). As shown in Table 2, α under HC was significantly inhibited by 21.1% ($p = 0.020$) at hyposaline and LI conditions compared to that under LC. Additionally, lower salinity significantly decreased the α under the HCLI condition ($p = 0.017$).

3.3. Pigment Contents

$p\text{CO}_2$ and the interaction with salinity had significant effects on the Chlorophyll *a* (Chl *a*) content in *P. yezoensis* (Table S3, $p = 0.035$, $p = 0.022$). Under the hyposaline condition, HC significantly increased the Chl *a* by 32.0% and 32.3% in the LI and II treatment groups, respectively (Figure 3, $p = 0.028$, $p = 0.028$). However, Chl *a* was not significantly changed by elevated $p\text{CO}_2$ at normal salinity regardless of light intensity (30 psu) ($p = 0.462$, $p = 0.310$), indicating that increasing salinity offset the boost of Chl *a* content. Carotenoids content showed a similar trend to Chl *a*, which was only significantly affected by the interaction of $p\text{CO}_2$ and salinity (Figure 4, $p = 0.016$).

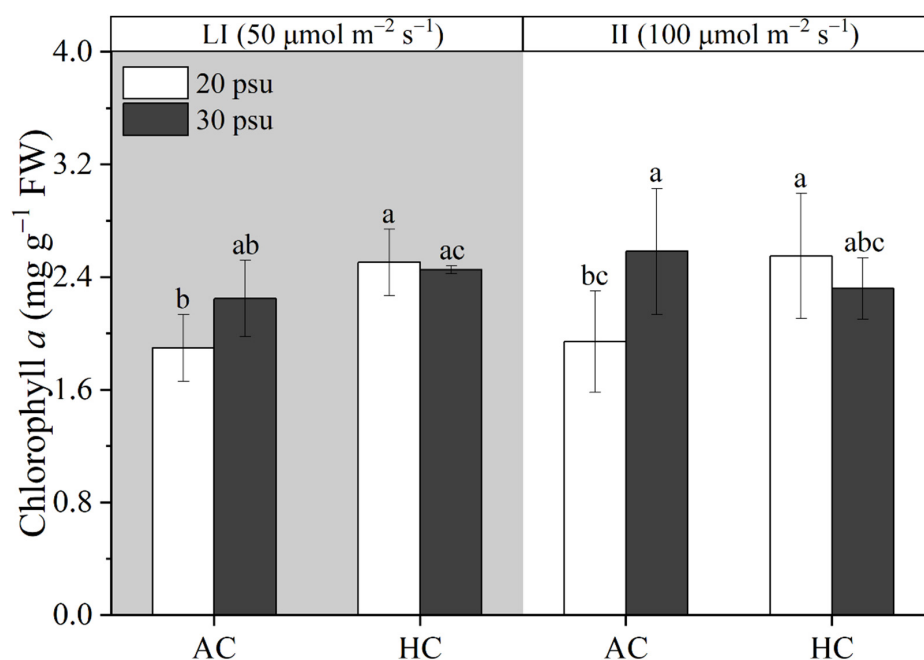


Figure 3. Changes in chlorophyll *a* contents of *Pyropia yezoensis* exposed to different salinities (20 and 30 psu) at different light intensities (50, 100 μmol photons m⁻² s⁻¹) treated under AC and HC conditions (AC, 400 μatm CO₂; HC, 1000 μatm CO₂). Results are expressed as the means ± SD (n = 3). Different letters indicate significant differences ($p < 0.05$) among the treatments.

3.4. Phycoerythrin Contents

Light intensity, salinity, and $p\text{CO}_2$ had no interactive effect, but the light had a significant effect on the phycoerythrin (PE) content of *P. yezoensis* (Table S3, $p < 0.001$). An increasing tendency was observed under the HC and AC conditions with increasing light intensity regardless of salinity (Figure 5). Under AC, the PE content in the II treatment was significantly enhanced by 50.7% and 56.1% compared to those under the LI condition ($p = 0.006$, $p = 0.006$). Under HC, the PE content in the II treatment was significantly enhanced by 69.2% and 32.4% compared to those under the LI condition ($p = 0.002$,

$p = 0.043$). The PE content of *P. yezoensis* showed a declining trend with the increase of CO₂ concentrations at the hyposaline condition, while the PE content showed the opposite trend at a salinity of 30 psu (Figure 5).

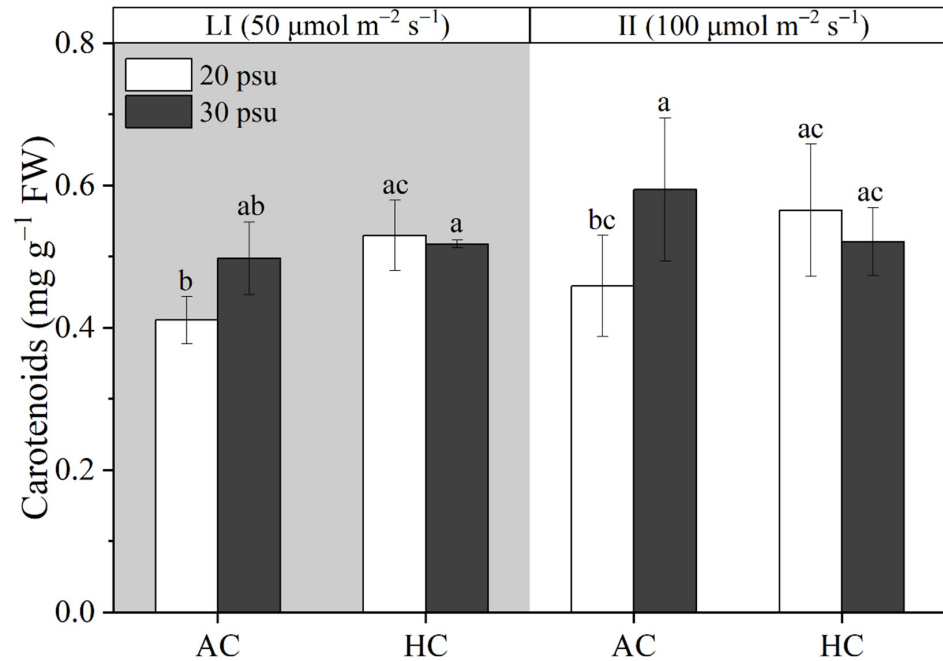


Figure 4. Changes in carotenoid contents of *Pyropia yezoensis* exposed to different salinities (20 and 30 psu) at different light intensities (50, 100 μmol photons m⁻² s⁻¹) treated under AC and HC conditions (AC, 400 μatm CO₂; HC, 1000 μatm CO₂). Results are expressed as the means ± SD (n = 3). Different letters indicate significant differences (p < 0.05) among the treatments.

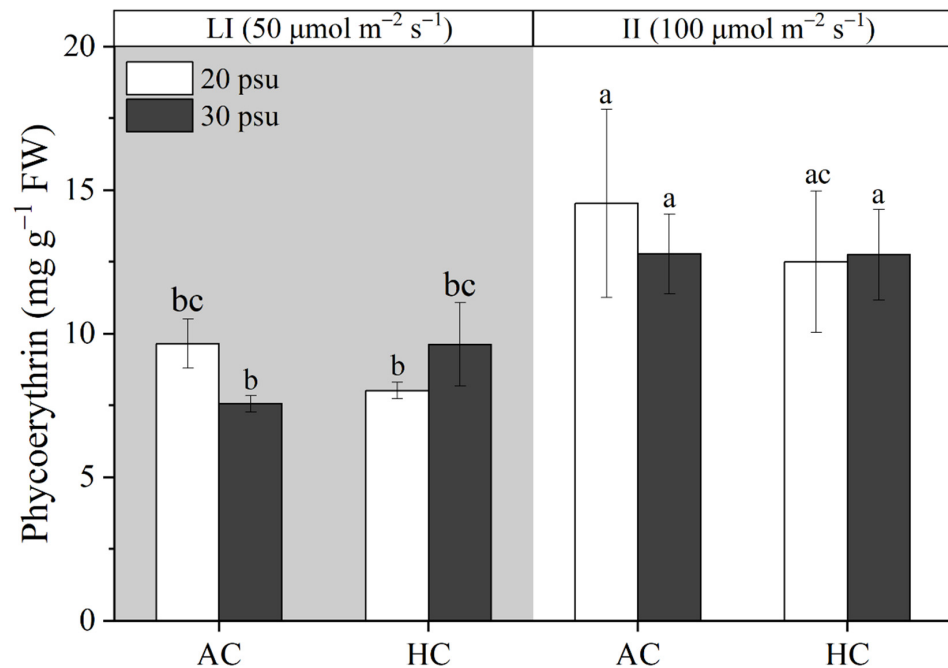


Figure 5. Changes in the phycoerythrin (PE) content of *Pyropia yezoensis* exposed to different salinities (20 and 30 psu) at different light intensities (50, 100 μmol photons m⁻² s⁻¹) treated under AC and HC conditions (AC, 400 μatm CO₂; HC, 1000 μatm CO₂). Results are expressed as the means ± SD (n = 3). Different letters indicate significant differences (p < 0.05) among the treatments.

3.5. Soluble Sugar Content

Light intensity, salinity, and CO₂ concentrations had no individual effect on the soluble sugar content (Table S4; $p = 0.583$, $p = 0.600$, $p = 0.579$), and the interaction between them was also not observed. Under the AC treatment, the content of soluble sugar under the hyposaline condition (20 psu) was decreased by 23.8% compared to that at normal salinity (30 psu), but there was no statistically significant difference (Figure 6, $p = 0.065$).

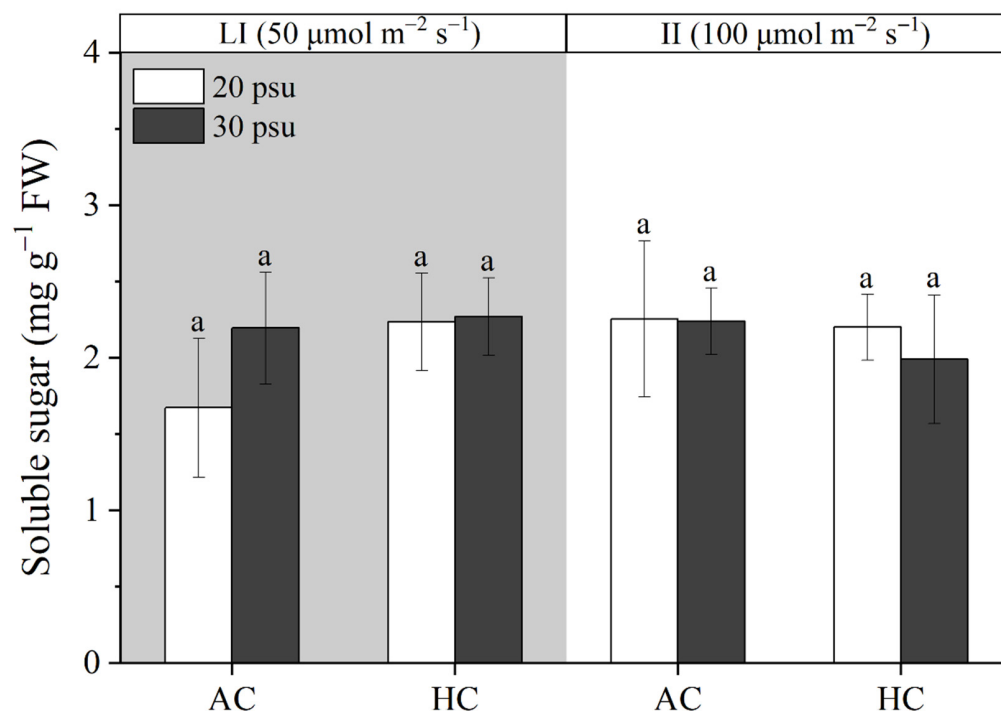


Figure 6. Changes in the soluble sugar content of *Pyropia yezoensis* exposed to different salinities (20 and 30 psu) at different light intensities (50, 100 μmol photons m⁻² s⁻¹) treated under AC and HC conditions (AC, 400 μatm CO₂; HC, 1000 μatm CO₂). Results are expressed as the means ± SD (n = 3). Different letters indicate significant differences ($p < 0.05$) among the treatments.

4. Discussions

Pyropia yezoensis is one of the most economically important seaweeds cultured in the intertidal zone and endures in a dramatically changing environment [42]. Therefore, *P. yezoensis* is often selected as a model macroalgae to study the impact of the environment on intertidal macroalgae. This study is the first attempt to investigate the combined influences of light, ocean acidification, and salinity stress on the physiology of *P. yezoensis*. In the present study, we found that *P. yezoensis* grew better under normal salinity (30 psu) than under the hyposaline condition (20 psu). In addition, intermediate irradiance increased the phycoerythrin content of thalli, ultimately enhancing the relative growth rate, which alleviated the stress caused by the low salinity in *P. yezoensis*.

Given that the intertidal zones where *Pyropia* species inhabit suffer terrestrial runoffs, the *Pyropia* species evolved a strong plasticity to the salinity fluctuations, which was verified by Li et al. by setting four salinity gradients [5]. Li et al. reported that there was a minor effect of salinity changes (17, 25, 32, 39 psu) on F_v/F_m in *P. yezoensis*. In addition, the F_v/F_m of *P. katadae* var. *hemiphylla* was also not significantly affected among the salinity fluctuations during 10 days of culture (15.6–50.6 psu) [43]. However, the rETR_{max} (electron transport rate), indicating the photosynthetic activity of PSII, was inhibited under hyposaline condition at each treatment in the present study (Table 2). Algal cells would adjust the turgor pressure to adapt to the hyposaline stress, resulting in the leakage of ions and electrolytes and changes in pH [44,45]. These changes can trigger a cascade of physiological processes and the accumulation of reactive oxygen species (ROS) [28,45].

Thus, *P. yezoensis* reallocate the energy to cope with the hyposaline stress, which leads to a decline in the biosynthesis of pigments under the AC condition (Figures 3 and 4). Although the low salinity decreased the growth of thalli, the difference was not statistically significant, suggesting that *P. yezoensis* exhibits a strong tolerance to salinity changes.

The effects of ocean acidification depend on the balance between the positive impact of increased CO₂ levels and the negative impact of reduced pH [22,46]. Moreover, the OA effect would also be influenced by other environmental stressors. It has been well documented that ocean acidification has different effects on the growth and photosynthesis of *P. yezoensis* and other macroalgae under different conditions [25,26,47,48]. In Bao et al.'s study, elevated *p*CO₂ significantly increased the growth of *P. yezoensis* under low light outdoors [25], and a similarly positive phenomenon was also observed at low light levels using cool white LEDs by Chen et al. [26]. Most macroalgae possess active CO₂-concentrating mechanisms (CCMs) to fulfill the demand for efficient photosynthesis [49]. At elevated *p*CO₂ levels, the energy saved by the down-regulation of CCM is reallocated for growth or other metabolic processes under light-limiting conditions [50]. In this work, elevated *p*CO₂ increased the contents of Chl *a* and Car. under hyposaline conditions but had no obvious effects at a salinity of 30 psu (Figures 3 and 4), indicating that ocean acidification could alleviate the hyposaline stress. Due to the enhancement of pigments, the growth of *P. yezoensis* was not significantly changed by elevated *p*CO₂ (Figure 1), which was described as a 'pigment economy' [51]. Low salinity generally reduces the rETR_{max} of *P. yezoensis*, resulting in limited energy utilized by thalli. Elevated *p*CO₂ increased the Chl *a* and Car contents in *P. yezoensis* to absorb light energy, but reduced the other pigments of the PE content due to different energy re-allocation strategies.

As a critical environmental factor, light could affect photosynthesis, pigment synthesis, substance accumulation, and the growth of macroalgae [10,52,53]. Phycoerythrin, as one of the light-harvesting proteins in red algae, absorbs light energy and transfers it efficiently to the reaction centers containing chlorophyll *a* [54]. In the present study, higher light intensity led to an increase in the PE content of *P. yezoensis*, thereby enhancing the energy absorption and ultimately promoting thalli growth, despite no significant changes observed in the contents of Chl *a* and Car. due to intermediate light intensity (Figures 1, 3 and 4). Furthermore, the negative effect of low salinity on the growth of thalli under 100 μmol photons m⁻² s⁻¹ was lower than that of 50 μmol photons m⁻² s⁻¹, indicating that *P. yezoensis* shows a higher tolerance to hyposaline condition with increasing light intensity (Figure 1). Although the soluble sugar content (mg g⁻¹ FW) does not change significantly (Figure 6), the soluble sugar production rate will be significantly affected because of the thalli growth is influenced by the light intensity (soluble sugar production rate = soluble sugar × relative growth rate).

In general, our findings demonstrate that *P. yezoensis* grew better at normal salinity than in hyposaline conditions. Additionally, intermediate light intensity increased phycoerythrin content, ultimately enhancing thalli growth, which mitigated hyposaline stress. Moreover, ocean acidification also alleviated hyposaline stress by promoting the pigment production of *P. yezoensis*. The study unveiled the complex interplay of these environmental factors and their impact on *P. yezoensis*. Future research could explore deeper into the molecular mechanisms governing these physiological responses, offering insights into the sustainable cultivation and conservation of this economically significant seaweed amidst environmental fluctuations.

Supplementary Materials: The following supporting information can be downloaded at: <https://www.mdpi.com/article/10.3390/jmse11112193/s1>, Table S1: Three-way analysis of variance (ANOVA) results in *Pyropia yezoensis* on the relative growth rate at different *p*CO₂ concentrations, light intensities, and salinity levels. df: degree of freedom; F: the value of F statistic; and Sig.: *p* value. Table S2: Three-way analysis of variance (ANOVA) results in *Pyropia yezoensis* on the chlorophyll fluorescence parameters at different *p*CO₂ concentrations, light intensities, and salinity levels. df: degree of freedom; F: the value of F statistic; and Sig.: *p* value. Table S3: Three-way analysis of variance (ANOVA) results in *Pyropia yezoensis* on the pigments at different *p*CO₂ concentrations, light intensities, and salinity levels. df: degree of freedom; F: the value of F statistic; and Sig.: *p* value.

Table S4: Three-way analysis of variance (ANOVA) results in *Pyropia yezoensis* on soluble sugar at different $p\text{CO}_2$ concentrations, light intensities, and salinity levels. df: degree of freedom; F: the value of F statistic; and Sig.: p value.

Author Contributions: Conceptualization, H.W. and H.L.; investigation, C.W., J.C., J.Z. and Z.L.; data curation, C.W., Z.L., F.C. and J.Z.; formal analysis, C.W. and J.C.; visualization, C.W. and H.L.; writing—original draft preparation, C.W. and J.X.; writing—review and editing, H.W., H.L. and J.X.; project administration, H.W.; funding acquisition, H.W. All authors have read and agreed to the published version of the manuscript.

Funding: This study was supported by the Natural Science Foundation of Jiangsu Province (grant number BK20221398), the National Natural Science Foundation of China (grant number 41706141), the “333” project of Jiangsu Province, the Jiang-su Planned Projects for Postdoctoral Research Funds (grant number 2018K025A), the “521 project” of Lianyungang city (grant number LYG06521202169), the “Haiyan project” of Lianyungang city (grant number 2018-ZD-005), the Open project of Jiangsu Institute of Marine Resources Development (grant number JSIMR202010), the “Huaguoshan project” of Lianyungang City, and the Lianyungang Planned Projects for Postdoctoral Research Funds.

Data Availability Statement: The data are available upon request to the corresponding author (Hailong Wu).

Conflicts of Interest: No potential financial or other interests could be perceived to influence the outcomes of the research. No conflicts, informed consent, human or animal rights applicable exist in the submission of this manuscript.

References

1. Wiencke, C.; Bischof, K. *Seaweed Biology: Novel Insights into Ecophysiology, Ecology and Utilization*; Springer Science & Business Media: Berlin, Germany, 2012; Volume 219.
2. Krause-Jensen, D.; Duarte, C.M. Substantial role of macroalgae in marine carbon sequestration. *Nat. Geosci.* **2016**, *9*, 737–742. [[CrossRef](#)]
3. Ortega, A.; Geraldi, N.R.; Alam, I.; Kamau, A.A.; Acinas, S.G.; Logares, R.; Gasol, J.M.; Massana, R.; Krause-Jensen, D.; Duarte, C.M. Important contribution of macroalgae to oceanic carbon sequestration. *Nat. Geosci.* **2019**, *12*, 748–754. [[CrossRef](#)]
4. Gao, G.; Clare, A.S.; Rose, C.; Caldwell, G.S. *Ulva rigida* in the future ocean: Potential for carbon capture, bioremediation and biomethane production. *Glob. Chang. Biol. Bioenergy* **2018**, *10*, 39–51. [[CrossRef](#)]
5. Li, X.; Sun, X.; Gao, L.; Xu, J.; Gao, G. Effects of periodical dehydration on biomass yield and biochemical composition of the edible red alga *Pyropia yezoensis* grown at different salinities. *Algal Res.* **2021**, *56*, 102315. [[CrossRef](#)]
6. Sutherland, J.E.; Lindstrom, S.C.; Nelson, W.A.; Brodie, J.; Lynch, M.D.; Hwang, M.S.; Choi, H.G.; Miyata, M.; Kikuchi, N.; Oliveira, M.C. A new look at an ancient order: Generic revision of the Bangiales (Rhodophyta). *J. Phycol.* **2011**, *47*, 1131–1151. [[CrossRef](#)] [[PubMed](#)]
7. FAO. *The State of World Fisheries and Aquaculture 2020. Sustainability in Action*; FAO: Rome, Italy, 2020. [[CrossRef](#)]
8. Zhang, T.; Li, J.; Ma, F.; Lu, Q.; Shen, Z.; Zhu, J. Study of photosynthetic characteristics of the *Pyropia yezoensis* thallus during the cultivation process. *J. Appl. Phycol.* **2014**, *26*, 859–865. [[CrossRef](#)]
9. Li, X.; Yang, L.; He, P.M. Formation and growth of free-living conchosporangia of *Porphyra yezoensis*: Effects of photoperiod, temperature and light intensity. *Aquac. Res.* **2011**, *42*, 1079–1086. [[CrossRef](#)]
10. Zhang, T.; Shen, Z.; Xu, P.; Zhu, J.; Lu, Q.; Shen, Y.; Wang, Y.; Yao, C.; Li, J.; Wang, Y. Analysis of photosynthetic pigments and chlorophyll fluorescence characteristics of different strains of *Porphyra yezoensis*. *J. Appl. Phycol.* **2012**, *24*, 881–886. [[CrossRef](#)]
11. Doney, S.C.; Busch, D.S.; Cooley, S.R.; Kroeker, K.J. The impacts of ocean acidification on marine ecosystems and reliant human communities. *Annu. Rev. Environ. Resour.* **2020**, *45*, 83–112. [[CrossRef](#)]
12. Gattuso, J.-P.; Magnan, A.; Billé, R.; Cheung, W.W.; Howes, E.L.; Joos, F.; Allemand, D.; Bopp, L.; Cooley, S.R.; Eakin, C.M. Contrasting futures for ocean and society from different anthropogenic CO₂ emissions scenarios. *Science* **2015**, *349*, aac4722. [[CrossRef](#)]
13. Orr, J.C.; Fabry, V.J.; Aumont, O.; Bopp, L.; Doney, S.C.; Feely, R.A.; Gnanadesikan, A.; Gruber, N.; Ishida, A.; Joos, F. Anthropogenic ocean acidification over the twenty-first century and its impact on calcifying organisms. *Nature* **2005**, *437*, 681–686. [[CrossRef](#)] [[PubMed](#)]
14. Cai, W.-J.; Hu, X.; Huang, W.-J.; Murrell, M.C.; Lehrter, J.C.; Lohrenz, S.E.; Chou, W.-C.; Zhai, W.; Hollibaugh, J.T.; Wang, Y. Acidification of subsurface coastal waters enhanced by eutrophication. *Nat. Geosci.* **2011**, *4*, 766–770. [[CrossRef](#)]
15. Ji, Y.; Xu, Z.; Zou, D.; Gao, K. Ecophysiological responses of marine macroalgae to climate change factors. *J. Appl. Phycol.* **2016**, *28*, 2953–2967. [[CrossRef](#)]
16. Sunday, J.M.; Fabricius, K.E.; Kroeker, K.J.; Anderson, K.M.; Brown, N.E.; Barry, J.P.; Connell, S.D.; Dupont, S.; Gaylord, B.; Hall-Spencer, J.M. Ocean acidification can mediate biodiversity shifts by changing biogenic habitat. *Nat. Clim. Chang.* **2017**, *7*, 81–85. [[CrossRef](#)]

17. Albright, R.; Takeshita, Y.; Koweek, D.A.; Ninokawa, A.; Wolfe, K.; Rivlin, T.; Nebuchina, Y.; Young, J.; Caldeira, K. Carbon dioxide addition to coral reef waters suppresses net community calcification. *Nature* **2018**, *555*, 516–519. [[CrossRef](#)]
18. Xu, D.; Schaum, C.E.; Lin, F.; Sun, K.; Munroe, J.R.; Zhang, X.W.; Fan, X.; Teng, L.H.; Wang, Y.T.; Zhuang, Z.M. Acclimation of bloom-forming and perennial seaweeds to elevated $p\text{CO}_2$ conserved across levels of environmental complexity. *Glob. Chang. Biol.* **2017**, *23*, 4828–4839. [[CrossRef](#)]
19. Gao, K.; Aruga, Y.; Asada, K.; Kiyohara, M. Influence of enhanced CO_2 on growth and photosynthesis of the red algae *Gracilaria* sp. and *G. chilensis*. *J. Appl. Phycol.* **1993**, *5*, 563–571. [[CrossRef](#)]
20. Zou, D.; Gao, K. Effects of elevated CO_2 on the red seaweed *Gracilaria lemaneiformis* (Gigartinales, Rhodophyta) grown at different irradiance levels. *Phycologia* **2009**, *48*, 510–517. [[CrossRef](#)]
21. Walker, B.J.; Strand, D.D.; Kramer, D.M.; Cousins, A.B. The response of cyclic electron flow around photosystem I to changes in photorespiration and nitrate assimilation. *Plant Physiol.* **2014**, *165*, 453–462. [[CrossRef](#)]
22. Li, H.; Beardall, J.; Gao, K. Photoinhibition of the picophytoplankter *Synechococcus* is exacerbated by ocean acidification. *Water* **2023**, *15*, 1228. [[CrossRef](#)]
23. Asada, K. Production and scavenging of reactive oxygen species in chloroplasts and their functions. *Plant Physiol.* **2006**, *141*, 391–396. [[CrossRef](#)] [[PubMed](#)]
24. Xie, X.; Lu, X.; Wang, L.; He, L.; Wang, G. High light intensity increases the concentrations of β -carotene and zeaxanthin in marine red macroalgae. *Algal Res.* **2020**, *47*, 101852. [[CrossRef](#)]
25. Bao, M.; Wang, J.; Xu, T.; Wu, H.; Li, X.; Xu, J. Rising CO_2 levels alter the responses of the red macroalga *Pyropia yezoensis* under light stress. *Aquaculture* **2019**, *501*, 325–330. [[CrossRef](#)]
26. Chen, C.; Zhang, Y.; Feng, Z.; Wu, M.; Xu, T.; Qiao, S.; Wang, W.; Ma, J.; Xu, J. Photosynthetic physiological response of *Porphyra yezoensis* to light change at different CO_2 concentrations. *Water* **2023**, *15*, 781. [[CrossRef](#)]
27. Lee, Y.-H.; Kim, D.-J.; Kim, H.-K. Characteristics of the seawater quality variation on the South Coastal Area of Korea. *KSCE J. Civ. Eng.* **2003**, *7*, 123–130. [[CrossRef](#)]
28. Karsten, U. Seaweed acclimation to salinity and desiccation stress. In *Seaweed Biology: Novel Insights into Ecophysiology, Ecology and Utilization*; Springer: Berlin/Heidelberg, Germany, 2012; pp. 87–107.
29. Wu, H.; Shin, S.K.; Jang, S.; Yarish, C.; Kim, J.K.; Wu, H.; Shin, S.K.; Jang, S.; Yarish, C.; Kim, J.K. Growth and nutrient bioextraction of *Gracilaria chorda*, *G. vermiculophylla*, *Ulva prolifera*, and *U. compressa* under hypo- and hyper-osmotic conditions. *Algae* **2018**, *33*, 329–340. [[CrossRef](#)]
30. Fong, P.; Boyer, K.E.; Desmond, J.S.; Zedler, J.B. Salinity stress, nitrogen competition, and facilitation: What controls seasonal succession of two opportunistic green macroalgae? *J. Exp. Mar. Biol. Ecol.* **1996**, *206*, 203–221. [[CrossRef](#)]
31. Kumar, M.; Kumari, P.; Gupta, V.; Reddy, C.; Jha, B. Biochemical responses of red alga *Gracilaria corticata* (Gracilariales, Rhodophyta) to salinity induced oxidative stress. *J. Exp. Mar. Biol. Ecol.* **2010**, *391*, 27–34. [[CrossRef](#)]
32. Samanta, P.; Shin, S.; Jang, S.; Kim, J.K. Comparative assessment of salinity tolerance based on physiological and biochemical performances in *Ulva australis* and *Pyropia yezoensis*. *Algal Res.* **2019**, *42*, 101590. [[CrossRef](#)]
33. Provasoli, L.J.C.; Algae, C.O. Media and prospects for the cultivation of marine algae. In *Cultures and Collections of Algae, Proceedings of United States and Japan Conference, Hakone, Japan, September 1966*; Japan Society of Plant Physiology: Tokyo, Japan, 1968; pp. 63–75.
34. Gao, G.; Qu, L.; Xu, T.; Burgess, J.G.; Li, X.; Xu, J. Future CO_2 -induced ocean acidification enhances resilience of a green tide alga to low-salinity stress. *ICES J. Mar. Sci.* **2019**, *76*, 2437–2445. [[CrossRef](#)]
35. Lewis, E.; Wallace, D. *Program Developed for CO_2 System Calculations*; Environmental System Science Data Infrastructure for a Virtual Ecosystem (ESS-DIVE): United States, 1998. Available online: <https://www.osti.gov/dataexplorer/biblio/dataset/1464255> (accessed on 18 October 2023).
36. Genty, B.; Briantais, J.-M.; Baker, N.R. The relationship between the quantum yield of photosynthetic electron transport and quenching of chlorophyll fluorescence. *Biochim. Biophys. Acta-Gen. Subj.* **1989**, *990*, 87–92. [[CrossRef](#)]
37. Eilers, P.; Peeters, J. A model for the relationship between light intensity and the rate of photosynthesis in phytoplankton. *Ecol. Model.* **1988**, *42*, 199–215. [[CrossRef](#)]
38. Jassby, A.D.; Platt, T. Mathematical formulation of the relationship between photosynthesis and light for phytoplankton. *Limnol. Oceanogr.* **1976**, *21*, 540–547. [[CrossRef](#)]
39. Wellburn, A.R. The spectral determination of chlorophylls *a* and *b*, as well as total carotenoids, using various solvents with spectrophotometers of different resolution. *J. Plant Physiol.* **1994**, *144*, 307–313. [[CrossRef](#)]
40. Beer, S.; Eshel, A. Determining phycoerythrin and phycocyanin concentrations in aqueous crude extracts of red algae. *Mar. Freshw. Res.* **1985**, *36*, 785. [[CrossRef](#)]
41. Loewus, F.A. Improvement in anthrone method for determination of carbohydrates. *Anal. Chem.* **1952**, *24*, 219. [[CrossRef](#)]
42. Blouin, N.A.; Brodie, J.A.; Grossman, A.C.; Xu, P.; Brawley, S.H. Porphyra: A marine crop shaped by stress. *Trends Plant Sci.* **2011**, *16*, 29–37. [[CrossRef](#)]
43. Wang, W.-J.; Sun, X.-T.; Liu, F.-L.; Liang, Z.-R.; Zhang, J.-H.; Wang, F.-J. Effect of abiotic stress on the gametophyte of *Pyropia katadae* var. *hemiphylla* (Bangiales, Rhodophyta). *J. Appl. Phycol.* **2016**, *28*, 469–479. [[CrossRef](#)]
44. Hurd, C.L.; Harrison, P.J.; Bischof, K.; Lobban, C.S. *Seaweed Ecology and Physiology*; Cambridge University Press: Cambridge, UK, 2014.

45. Kumar, M.; Kumari, P.; Reddy, C.; Jha, B. Salinity and desiccation induced oxidative stress acclimation in seaweeds. In *Advances in Botanical Research*; Elsevier: Amsterdam, The Netherlands, 2014; Volume 71, pp. 91–123.
46. Qu, L.; Beardall, J.; Jiang, X.; Gao, K. Elevated $p\text{CO}_2$ enhances under light but reduces in darkness the growth rate of a diatom, with implications for the fate of phytoplankton below the photic zone. *Limnol. Oceanogr.* **2021**, *66*, 3630–3642. [[CrossRef](#)]
47. Liu, C.; Zou, D.; Yang, Y. Comparative physiological behaviors of *Ulva lactuca* and *Gracilariopsis lemaneiformis* in responses to elevated atmospheric CO_2 and temperature. *Environ. Sci. Pollut. Res.* **2018**, *25*, 27493–27502. [[CrossRef](#)]
48. Liu, C.; Zou, D.; Liu, Z.; Ye, C. Ocean warming alters the responses to eutrophication in a commercially farmed seaweed, *Gracilariopsis lemaneiformis*. *Hydrobiologia* **2020**, *847*, 879–893. [[CrossRef](#)]
49. Raven, J.A.; Hurd, C.L. Ecophysiology of photosynthesis in macroalgae. *Photosynth. Res.* **2012**, *113*, 105–125. [[CrossRef](#)]
50. Olischläger, M.; Wiencke, C. Ocean acidification alleviates low-temperature effects on growth and photosynthesis of the red alga *Neosiphonia harveyi* (Rhodophyta). *J. Exp. Bot.* **2013**, *64*, 5587–5597. [[CrossRef](#)] [[PubMed](#)]
51. Gao, G.; Gao, Q.; Bao, M.; Xu, J.; Li, X. Nitrogen availability modulates the effects of ocean acidification on biomass yield and food quality of a marine crop *Pyropia yezoensis*. *Food Chem.* **2019**, *271*, 623–629. [[CrossRef](#)] [[PubMed](#)]
52. Wu, H.; Jiang, H.; Liu, C.; Deng, Y. Growth, pigment composition, chlorophyll fluorescence and antioxidant defenses in the red alga *Gracilaria lemaneiformis* (Gracilariales, Rhodophyta) under light stress. *S. Afr. J. Bot.* **2015**, *100*, 27–32. [[CrossRef](#)]
53. Zou, D.; Gao, K. Photosynthetic acclimation to different light levels in the brown marine macroalga, *Hizikia fusiformis* (Sargassaceae, Phaeophyta). *J. Appl. Phycol.* **2010**, *22*, 395–404. [[CrossRef](#)]
54. Sfriso, A.A.; Gallo, M.; Baldi, F. Phycoerythrin productivity and diversity from five red macroalgae. *J. Appl. Phycol.* **2018**, *30*, 2523–2531. [[CrossRef](#)]

Disclaimer/Publisher’s Note: The statements, opinions and data contained in all publications are solely those of the individual author(s) and contributor(s) and not of MDPI and/or the editor(s). MDPI and/or the editor(s) disclaim responsibility for any injury to people or property resulting from any ideas, methods, instructions or products referred to in the content.